JOC Article

Imidazole-Annelated Ferrocene Derivatives as Highly Selective and Sensitive Multichannel Chemical Probes for Pb(II) Cations

Fabiola Zapata, Antonio Caballero, Arturo Espinosa, Alberto Tárraga,* and Pedro Molina*

Departamento de Química Orgánica, Facultad de Química, Universidad de Murcia, Campus de Espinardo, E-30100 Murcia, Spain

pmolina@um.es; atarraga@um.es

Received March 12, 2009

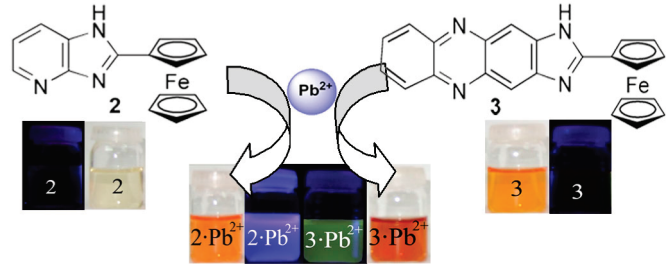

New ferrocenyl-containing imidazopyridine and imidazophenazine receptors **2**−**5** show high selective affinity for Pb(II) ions over a range of other metal ions examined through different channels. Imidazopyridine−ferrocene dyad **2** behaves as a highly selective redox, chromogenic, and fluorescent chemosensor molecule for Pb^{2+} cations: the oxidation redox peak is anodically shifted ($\Delta E_{1/2}$ = 150 mV), and the low energy band of the absorption spectrum is red-shifted ($\Delta\lambda$ = 44 nm) upon complexation with this metal cation. This change in the absorption spectrum is accompanied by a color change from colorless to orange, which allows the potential for "naked eye" detection. The emission spectrum undergoes an important chelation-enhanced fluorescence (CHEF) effect (CHEF = 620), with an unprecedented detection limit of 2.7 μg L^{-1}. The presence of Zn^{2+} cations also induced a perturbation of the redox potential, absorption, and emission spectra although in less extension than those found with Pb^{2+} cations. Imidazophenazine−ferrocene dyad **3** has also shown its ability for sensing Pb^{2+} cations through redox ($\Delta E_{1/2}$ = 120 mV), absorption ($\Delta\lambda$ = 23 nm), and emission (CHEF = 133) channels, whereas the presence of Zn^{2+} only has a little effect on the emission spectrum (CHEF = 74). The electrochemical changes observed in the two-armed ferrocenes **4** and **5** upon complexation show that the potential shift is higher for Zn^{2+} ions ($\Delta E_{1/2}$ = 190−170 mV) than for Pb^{2+} ions ($\Delta E_{1/2}$ = 180−110 mV), which is in clear contrast to those observed for the monoarmed ferrocenes **2** and **3**. The recognition properties of the two-armed imidazopyridine−ferrocene triad **4** are quite similar to those exhibited by the parent monosubstituted receptor **2**, and the most salient features are a strong perturbation of the redox wave ($\Delta E_{1/2}$ = 180 mV), a dramatic increasing of the fluorescent quantum yield ($\Phi_{complex}/\Phi_{ligand}$ = 890) in the presence of Pb^{2+}, while the optical responses toward Zn^{2+} cations were silent. The two-armed imidazophenazine−ferrocene triad **5** senses Pb^{2+} cations through perturbation of the oxidation potential of the Fe(II)/Fe(III) redox couple ($\Delta E_{1/2}$ = 110 mV), important blue shift ($\Delta\lambda$ = 160 nm) of the high energy band in the absorption spectrum, and a remarkable increase of the emission band (CHEF = 220), whereas smaller changes were observed in the presence of Zn^{2+} cations. ^{1}H NMR studies as well as DFT calculations have been carried out to get information about which molecular sites are involved in the binding event.

Introduction

Among heavy metal, lead is the most abundant and ranks second in the list of toxic substances and is often encountered due to its wide distribution in the environment as well as its current and previous use in batteries, gasoline, and pigments. Lead pollution is an ongoing danger to the human health, particularly in children (memory loss, irritability, anemia, muscle paralysis, and mental retardation),[1] and the environment, as most of the 300 million tons of this heavy metal mined to date are still circulating in soil and groundwater.[2] Despite effort to reduce global emissions, lead poisoning remains the world's most

(1) Lin-Fu, J. S. Lead Poisoning, A Century of Discovery and Rediscovery. In *Human Lead Exposure*; Needleman, H. L., Ed.; Lewis Publishing: Boca Raton, FL, 1992.

(2) Flegal, A. R.; Smith, D. R. *Environ. Res.* **1992**, *58*, 125–133.

10.1021/jo900533x CCC: $40.75
Published on Web 06/01/2009

common environmentally caused disease.[3] Thus, the level of this detrimental ion, which is present in tap water as a result of dissolution from household plumbing systems, is the object of several official norms. The World Health Organization established in 1996 a guideline for drinking-water quality,[4] which included a lead maximal value of 10 mg L^{-1}. Thus, keeping in view the role of Pb^{2+}, the detection and monitoring of this metal cation by methods which allow the development of selective and sensitive assays becomes very important. As many heavy metals are known as fluorescence quenchers via enhanced spin−orbital coupling,[5] energy or electron transfer,[6] development of fluorescent sensors for Pb^{2+} presents a challenge. In this context, considerable efforts have been undertaken to develop fluorescent chemosensors for Pb^{2+} ions based on peptide,[7] protein,[8] DNAzyme,[9] polymer,[10] and small-molecule[11] scaffolds. There is, however, a paucity of use of multichannel receptors as potential guest reporters via multiple signaling patterns. Specifically, as we report here, the development of multichannel (chromogenic/fluorogenic/electrochemical) Pb^{2+} selective chemosensors is, as far as we know, an unexplored subject,[12] and only three dual chromogenic and redox receptors have been recently described.[13]

Among the various abiotic receptors reported in the literature, those employing benzimidazole derivatives as anion-binding motif have attracted considerable attention very recently.[14] In this sense, we have reported that the imidazophenanthroline ring system displays interesting anion-sensing properties, which can be modulated by metal cation coordination.[15] In this line, it seems to be of interest to study how the binding properties of the benzimidazole core may be not only modulated but also changed either by introduction of an additional heterocycle nitrogen atom at an appropriate position in the six-membered ring or by linear annelation to aza-heterocycles leading to expanded benzimidazole derivatives bearing several binding sites.

Surprisingly and as far as we know, imidazo[4,5-*b*]pyridines (1-deazapurines) have never been used for sensing purposes, despite their easy synthesis,[16] photophysical properties,[17] and biological applications.[18] On the other hand, the phenazine ring is of interest in the construction of molecular assemblies of metals because it acts as monodentate ligand as well as an electron donor.[19] In this context, only two examples of the phenazine ring system[20] have been reported in ion recognition processes: a phenazine-based urea/thiourea derivative used as a chromogenic receptor for anions[21] and a dibenzopyridophenazine derivative used as a fluorescent lithium chemosensor molecule.[22] In addition, the phenazine derivative, imidazo[4,5-*b*]phenazine, has been prepared with the aim of searching for new efficient fluorescent probes to study biological processes and for new luminescent analogues of some biologically active molecules.[23] On the other hand, in ferrocene derivatives, cation binding at an adjacent receptor site induces a positive shift in the redox potential of the ferrocene/ferrocenium redox couple, and the complexation ability of the ligand can be switched on and off by varying the applied electrochemical potential. The magnitude of the electrochemical shift ($\Delta E_{1/2}$) upon complexation represents a quantitative measure of the perturbation of the redox center induced by complexation to the receptor unit.[24] Binding at a proximate site can also affect the UV−vis properties of the ferrocene unit. In general, complexation induces bathochromic shifts in the lower energy spin-allowed ferrocene absorption band, which is between 400 and 500 nm.[25] The field of research dealing with fluorescent ferrocene-based chemosensor molecules is still in its infancy, probably because ferrocene derivatives are known to be efficient fluorescence quenchers.[26] However, it is also established that incorporating

(3) Claudio, E. S.; Godwin, H. A.; Magyar, J. S. *Prog. Inorg. Chem.* **2003**, *51*, 1–144, and references therein.
(4) *Guidelines for Drinking-Water Quality, Geneva*, 2nd ed.; World Health Organization, 1996; Vol. 2, p 940.
(5) McClure, D. S. *J. Chem. Phys.* **1952**, *20*, 682–686.
(6) Varnes, A. W.; Dodson, R. B.; Whery, E. L. *J. Am. Chem. Soc.* **1972**, *94*, 946–950.
(7) Deo, S.; Godwin, H. A. *J. Am. Chem. Soc.* **2000**, *122*, 174–175.
(8) Chen, P.; Greenberg, B.; Taghvi, S.; Romano, C.; van der Lelie, D.; He, C. *Angew. Chem., Int. Ed.* **2005**, *44*, 2715–2719.
(9) (a) Liu, J.; Lu, Y. *J. Am. Chem. Soc.* **2000**, *122*, 10466–10467. (b) Liu, J.; Lu, Y. *J. Am. Chem. Soc.* **2003**, *125*, 6642–6643. (c) Liu, J.; Lu, Y. *J. Am. Chem. Soc.* **2004**, *126*, 12298–12305. (d) Chang, I. H.; Tulock, J. J.; Liu, J.; Kim, W.-S.; Cannon, D. M., Jr.; Lu, Y.; Bohn, P. W.; Sweedler, J. V.; Cropek, D. M. *Environ. Sci. Technol.* **2005**, *39*, 3756–3761.
(10) Kim, I.-K.; Dunkhorst, A.; Gilbert, J.; Bunz, U. H. F. *Macromolecules* **2005**, *38*, 4560–4562.
(11) (a) Kwon, J. Y.; Jang, Y. J.; Lee, Y. J.; Kim, K. M.; Seo, M. S.; Nam, W.; Yoon, J. *J. Am. Chem. Soc.* **2005**, *127*, 10107–10111. (b) Kavallieratos, K.; Rosenberg, J. M.; Chen, W.-Z.; Ren, T. *J. Am. Chem. Soc.* **2005**, *127*, 6514–6515. (c) Lee, J. Y.; Kim, S. K.; Jung, J. H.; Kim, J. S. *J. Org. Chem.* **2005**, *70*, 1463–1466. (d) Liu, J.-M.; Bu, J.-H.; Zheng, Q.-Y.; Chen, C.-F.; Huang, Z.-T. *Tetrahedron Lett.* **2006**, *47*, 1905–1908. (e) Metivier, R.; Leray, I.; Valeur, B. *Chem. Commun.* **2003**, 996–997. (f) Metivier, R.; Leray, I.; Valeur, B. *Chem.—Eur. J.* **2004**, *10*, 4480–4490. (g) Chen, C.-T.; Huang, W.-P. *J. Am. Chem. Soc.* **2002**, *124*, 6246–6247. (h) Ma, L.-J.; Liu, Y.-F.; Wu, Y. *Chem. Commun.* **2006**, 2702–2704. (i) Wu, F.-Y.; Bae, S. W.; Hong, J.-I. *Tetrahedron Lett.* **2006**, *47*, 851–8854. (j) He, Q.; Miller, E. W.; Wong, A. P.; Chang, C. J. *J. Am. Chem. Soc.* **2006**, *128*, 9316–9317. (k) Crego-Calama, M.; Reinhoudt, D. N. *Adv. Mater.* **2001**, *13*, 1171–1174. (l) Lee, J. Y.; Kim, S. K.; Jung, J. H.; Kim, J. S. *J. Org. Chem.* **2005**, *70*, 1463–1466.
(12) For a preliminary communication, see: Zapata, F.; Caballero, A.; Espinosa, A.; Tárraga, A.; Molina, P. *Org. Lett.* **2008**, *10*, 41–44.
(13) (a) Xue, H.; Tang, X.-J.; Wu, L.-Z.; Zhang, L.-P.; Tung, C.-H. *J. Org. Chem.* **2005**, *70*, 9727–9734. (b) Remeter, D.; Blanchard, P.; Allain, M.; Grosu, I.; Roncali, J. *J. Org. Chem.* **2007**, *72*, 5285–5290. (c) Caballero, A.; Espinosa, A.; Tárraga, A.; Molina, P. *J. Org. Chem.* **2008**, *73*, 5489–5497.
(14) (a) Kang, J.; Kim, H. S.; Jang, D. O. *Tetrahedron Lett.* **2005**, *46*, 6079–6082. (b) Bai, Y.; Zhang, B.-G.; Xu, J.; Duan, C.-Y.; Dang, D.-B.; Liu, D.-J.; Meng, Q.-J. *New J. Chem.* **2005**, *29*, 777–779. (c) Moon, K. S.; Singh, N.; Lee, G. W.; Jang, D. O. *Tetrahedron* **2007**, *63*, 9106–9111. (d) Singh, N.; Jang, D. O. *Org. Lett.* **2007**, *9*, 1991–1994. (e) Yu, M.; Ln, H.; Zhao, G.; Lin, H. *J. Mol. Recognit.* **2007**, *20*, 69–73.
(15) Zapata, F.; Caballero, A.; Espinosa, A.; Tárraga, A.; Molina, P. *J. Org. Chem.* **2008**, *73*, 4034–4044.
(16) Yutilov, Y. M. *Adv. Heterocycl. Chem.* **2005**, *89*, 159–270.
(17) (a) Adler, T. K. *Anal. Chem.* **1962**, *34*, 685–689. (b) Das, S. K.; Dogra, S. K. *J. Chem. Soc., Perkin Trans. 2* **1998**, 2765–2771.
(18) (a) Heitsch, H.; Becker, R. H. A.; Kleemann, H.-W.; Wagner, A. *Bioorg. Med. Chem.* **1997**, *5*, 673–678. (b) Dubey, P. K.; Kumar, R. V.; Naidu, A.; Kulkarni, S. M. *Asian J. Chem.* **2002**, *14*, 1129–1152.
(19) Munakata, M.; Kitagawa, S.; Ujimaru, N.; Nakamura, M.; Maekawa, M.; Matsuda, H. *Inorg. Chem.* **1993**, *32*, 826–832.
(20) The redox-active phenazines are heteroaromatic dyes, which are widely employed in biology and medicine for staining of submolecular particles and tissues. For a recent review, see: Laursen, J. B.; Nielsen, J. *Chem. Rev.* **2004**, *104*, 1663–1685.
(21) Chauhan, S. M. S.; Bisht, T.; Garg, B. *Tetrahedron Lett.* **2008**, *49*, 6646–6649.
(22) Obare, S. O.; Murphy, C. J. *Inorg. Chem.* **2001**, *40*, 6080–6082.
(23) Makitruk, V. L.; Yarmoluk, S. N.; Shalamay, A. S.; Alexeeva, I. V. *Nucleic Acids Res.* **1991**, *24*, 244.
(24) (a) López, J. L.; Tárraga, A.; Espinosa, A.; Velasco, M. D.; Molina, P.; Lloveras, V.; Vidal-Gancedo, J.; Rovira, C.; Veciana, J.; Evans, D. J.; Wurst, K. *Chem.—Eur. J.* **2004**, *10*, 1815–1826. (b) Caballero, A.; Martinez, R.; Lloveras, V.; Ratera, I.; Vidal-Gancedo, J.; Wurst, K.; Tárraga, A.; Molina, P.; Veciana, J. *J. Am. Chem. Soc.* **2005**, *127*, 15666–15667. (c) Martínez, R.; Espinosa, A.; Tárraga, A.; Molina, P. *Org. Lett.* **2005**, *7*, 5869–5872. (d) Caballero, A.; Lloveras, V.; Curiel, D.; Tárraga, A.; Espinosa, A.; Garcia, R.; Vidal-Gancedo, J.; Rovira, C.; Wurst, K.; Molina, P.; Veciana, J. *Inorg. Chem.* **2007**, *46*, 825–838. (e) Zapata, F.; Caballero, A.; Espinosa, A.; Tárraga, A.; Molina, P. *Org. Lett.* **2007**, *9*, 2385–2388.
(25) (a) Beer, P. D.; Smith, D. K. *J. Chem. Soc., Dalton Trans.* **1998**, 417–423. (b) Carr, J. D.; Coles, S. J.; Hassan, W. W.; Hursthouse, M. B.; Malik, K. M. A.; Tucker, J. H. R. *J. Chem. Soc., Dalton Trans.* **1999**, 57–62. (c) Barlow, S.; Bunting, H. E.; Ringham, C.; Green, J. C.; Bublitz, G. U.; Boxer, S. G.; Perry, J. W.; Marder, S. R. *J. Am. Chem. Soc.* **1999**, *121*, 3715–3723.
(26) Fery-Forgues, S.; Delavaux-Nicot, B. *J. Photochem. Photobiol. A* **2000**, *132*, 137–159.

SCHEME 1. Synthesis of 2-Ferrocenylimidazo Derivatives 1−5[a]

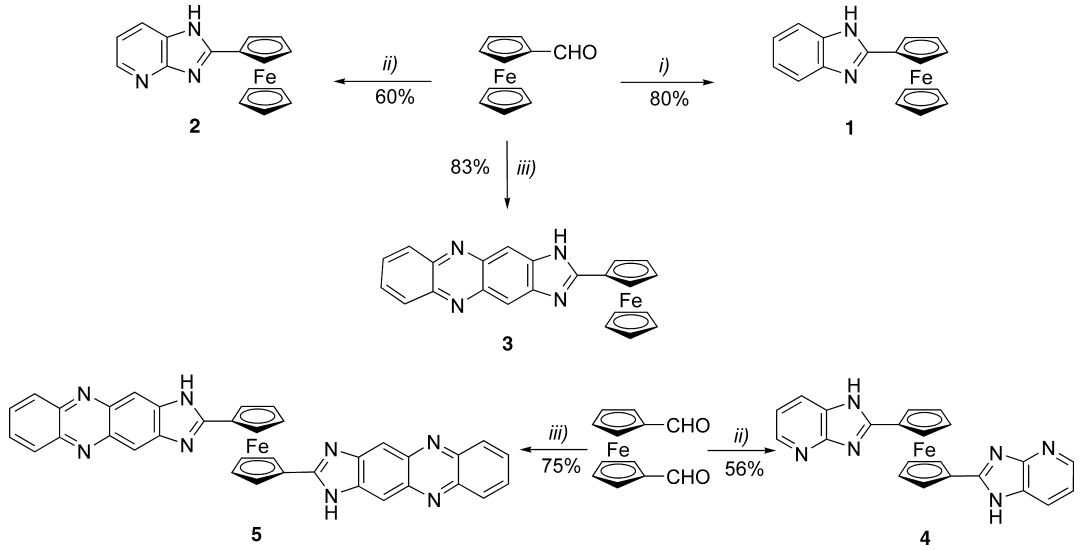

[a] Reagents and conditions: (i) 1,2-diaminobenzene, nitrobenzene, 60°C, 15 h; (ii) 2,3-diaminopyridine, nitrobenzene, 60°C, 15 h; (iii) 2,3-diaminophenazine, nitrobenzene, 60°C, 15 h.

a ferrocenyl derivative into a luminescent system does not necessarily extinguish the luminescence.[27]

On the basis of this body of work, we decided to combine the redox activity of the ferrocene group with the photoactive behavior and binding ability of imidazo-fused heterocycles. In the context of this work, it has been found that the introduction of either an additional nitrogen atom in the six-membered ring of the benzimidazole ring, with similar basicity to that of the imidazole nitrogen, imparts an interesting behavior as the pyridine-like nitrogen atom of the six-membered ring could cooperate with the basic nitrogen of the imidazole ring or a linear-fused quinoxaline ring could promote the binding affinity of these ring systems toward metal cations. To this end, the mono- and two-armed 2-ferrocenyl-imidazo[4,5-*b*]pyridines **2** and **4** and 2-ferrocenylimidazo[4,5-*b*]phenazines **3** and **5** have been chosen to develop multiple-channel systems, where the fluorescent reporter is integrated with and the redox unit is linked to the guest cation binding site. The synthesis of the new compounds is described, and an analysis of their cation complexing properties by optical (absorption and emission) spectroscopy, ^{1}H NMR spectroscopy, mass spectrometry, and electrochemical measurements is presented.

Results and Discussion

Synthesis. Preparation of the target compounds **1**−**3** has been achieved by reaction of the appropriate *o*-arylene diamine with formylferrocene in the presence of nitrobenzene as oxidizing agent,[28] whereas 1,1′-diformylferrocene[29] has been used as a carbonyl component for the preparation two-armed ferrocene derivatives **4** and **5** (Scheme 1).

Redox and Optical Properties. The reversibility and the relative oxidation potential of the ferrocene/ferrocenium redox couple in receptors **1**−**5** were determined by cyclic voltammetry (CV) and Osteryoung square-wave voltammetry (OSWV) in CH_3CN solutions containing 0.1 M $[(n\text{-}Bu)_4N]ClO_4$ as supporting electrolyte. All processes observed were reversible, according to the criteria of (i) separation of 60 mV between cathodic and anodic peaks, (ii) close-to-unity ratio of the intensities of the cathodic and anodic currents, and (iii) constancy of the peak potential on changing sweep rate in the CVs. The same half-wave potential values have been obtained from the OSWV peaks and from an average of the cathodic and anodic cyclic voltammetric peaks. As expected, monosubstituted ferrocene ligands **1**−**3** display a reversible one-electron oxidation process at $E_{1/2} = 0.58-0.64$ V versus decamethylferrocene, due to the ferrocene/ferrocenium redox couple. Likewise, the 1,1′-disubstituted ferrocenes **4** and **5** also showed a reversible oxidation wave at $E_{1/2} = 0.71$ V for **4** and $E_{1/2} = 0.78$ for **5** versus decamethylferrocene. Looking at the formal oxidation potentials of monosubstituted **1**−**3** versus disubstituted ferrocenes **4** and **5**, the higher electron-withdrawing character of the two fused aza-heterocyclic moieties results in an increase of the oxidation potential for the disubstituted ferrocenyl imidazole derivatives when compared to the corresponding monosubstituted one (Table 1).

In general, absorption spectra of these ligands were carried out in CH_3CN solutions (see table in the Supporting Information), and interestingly, those obtained for ligands **1**−**3** are similar to those reported for imidazo[4,5-*b*]pyridine[30] and imidazo[4,5-*b*]phenazine[31] derivatives. The absorption spectra of ligands **1** and **2** are almost identical. The spectrum of the receptor **1** displays a strong high energy (HE) band at 305 nm ($\varepsilon = 22\,400$ M^{-1} cm^{-1}) and a broad low energy (LE) band of lower intensity at 457 nm ($\varepsilon = 660$ M^{-1} cm^{-1}). Likewise, the spectrum of the receptor **2** shows two bands at 309 nm ($\varepsilon = 24\,600$ M^{-1} cm^{-1}) and at 448 nm ($\varepsilon = 1010$ M^{-1} cm^{-1}). However, a blue-shifted HE band at 292 nm ($\varepsilon = 22\,500$ M^{-1}

(27) Molina, P.; Tárraga, A.; Caballero, A. *Eur. J. Inorg. Chem.* **2008**, 3401–3417.

(28) (a) Preston, P. N. *Chem. Rev.* **1974**, *74*, 279–314. (b) Chang, L. C. W.; von Frijtag Drabbe Künzel, J. K.; Mulder-Krieger, T.; Westerhout, J.; Spangenberg, T.; Brusse, J.; IJzerman, A. P. *J. Med. Chem.* **2007**, *50*, 828–834. (c) Kus, C.; Ayhan-Kilcigil, G.; Özbey, S.; Kaynak, F. B.; Kaya, M.; Çoban, T.; Can-Eke, B. *Bioorg. Med. Chem.* **2008**, *16*, 4294–4303. (d) Mayence, A.; Pietka, A.; Collins, M. S.; Cushion, M. T.; Tekwani, B. L.; Huang, T. L.; Vanden Eynde, J. J. *Bioorg. Med. Chem.* **2008**, *18*, 2658–2661.

(29) Sanders, R.; Mueller-Westerhoff, U. T. *J. Organomet. Chem.* **1996**, *512*, 219–224.

(30) Das, S. K.; Dogra, S. K. *J. Chem. Soc., Perkin Trans. 2* **1998**, 2765–2771.

(31) Ryazanova, O. A.; Voloshin, I. M.; Makitruk, V. L.; Zozulya, V. N.; Karachevtsev, V. A. *Spectrochim. Acta, Part A* **2007**, *66*, 849–859.

TABLE 1. Electrochemical Data of the Receptors 1−5 and Their Metal Complexes Formed

compound	$E_{1/2}$ (mV)	ΔE (mV)[a]	K_{ox}/K_{red} (BEF)[b]
1	580	–	–
1·Pb^{2+}	830	250	5.9×10^{-5}
1·Zn^{2+}	830	250	5.9×10^{-5}
1·Hg^{2+}	830	250	5.9×10^{-5}
2	590	–	–
2·Pb^{2+}	740	150	2.9×10^{-3}
2·Zn^{2+}	680	090	3×10^{-2}
2·Hg^{2+}	710	120	9.4×10^{-3}
3	640	–	–
3·Pb^{2+}	760	120	9.4×10^{-3}
4	710	–	–
4·Pb^{2+}	890	180	9×10^{-4}
4·Zn^{2+}	900	190	6.13×10^{-4}
5	780	–	–
5·Pb^{2+}	890	110	1.3×10^{-2}
5·Zn^{2+}	950	170	1.3×10^{-3}

[a] $\Delta E = E_{1/2}$(complex) − $E_{1/2}$(free ligand). [b] BEF = Binding enhancement factor, calculated using the equation $\Delta E^{\circ} = nF/RT \ln(K_{ox}/K_{red})$, where the equilibrium constants K_{ox} and K_{red} correspond to the complexation processes by the oxidized and reduced forms of the ligand.

cm^{-1}) and a red-shifted LE band at 503 nm ($\epsilon = 5740$ M^{-1} cm^{-1}) are present in the absorption spectrum of receptor **3** along with a prominent band at 386 nm ($\varepsilon = 16\,800$ M^{-1} cm^{-1}). Absorption spectrum of the 1,1′-disubstituted ferrocene **4** is similar to that exhibited by the pararent monosubstituted **2**; it displays a strong absorption band at 303 nm ($\varepsilon = 22\,800$ M^{-1} cm^{-1}) and a less and broad band at 457 nm ($\varepsilon = 580$ M^{-1} cm^{-1}). Disubstituted receptor **5** exhibits a high energy band at 260 nm ($\varepsilon = 14\,500$ M^{-1} cm^{-1}) and a red-shifted low energy band at 573 nm ($\varepsilon = 3100$ M^{-1} cm^{-1}), between them a broad band at 397 nm ($\varepsilon = 4900$ M^{-1} cm^{-1}) is present.

Receptors **2** and **4**, bearing one or two imidazopyridine substituents, exhibit very weak fluorescence in CH_3CN ($c = 10^{-5}$ M), with the excitation spectrum revealing $\lambda_{exc} = 330$ and 360 nm for **2** and **4**, respectively, as an ideal excitation wavelength. The emission spectra show two broad and structureless bands at 364 and 377 nm due to the 1-deazapurine ring, with rather low quantum yield[17a] ($\Phi = 3.92 \times 10^{-4}$). Likewise, the fluorescence spectrum of receptors **3** and **5** bearing one or two imidazophenazine rings represents a broad unstructured band with a maximum at 535 nm ($\lambda_{exc} = 410$ nm) with low rather fluorescent quantum yield ($\Phi = 5.88 \times 10^{-4}$ for both **3** and **5**).

Ion Sensing Properties. The metal cation complexing properties of receptors **1**−**5** toward Li^+, Na^+, K^+, Ca^{2+}, Mg^{2+}, Ni^{2+}, Pb^{2+}, Zn^{2+}, Hg^{2+}, and Cd^{2+} have been investigated by electrochemistry, spectroscopic measurements, and ^{1}H NMR spectroscopy. In general, the results show that the univalent metal ions do not cause significant changes in either redox potential, absorption, or the fluorescence emission spectrum, whereas redox shift, red-shifted absorptions, and increased emission bands are observed upon the addition of Pb^{2+}, Zn^{2+}, and Hg^{2+} metal cations.

Addition of Pb^{2+}, Zn^{2+}, or Hg^{2+} ions to an electrochemical solution of the receptor **1** induced an anodic shift of the oxidation potential from $E_{1/2} = 0.58$ V to $E_{1/2} = 0.83$ V ($\Delta E_{1/2} = 250$ mV). On stepwise addition of Pb^{2+} ions to a solution of the receptor **2**, a clear evolution of the oxidation wave from $E_{1/2} = 0.59$ V to $E_{1/2} = 0.74$ V ($\Delta E_{1/2} = 150$ mV) was observed, and maximum perturbation of the CV was obtained with 1 equiv of added Pb^{2+} ions (Figure 1).

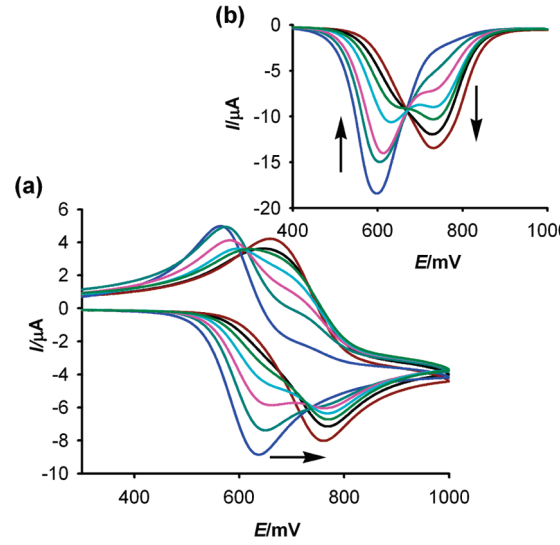

FIGURE 1. Evolution of the CV (a) and OSWV (b) of receptor **2** (1 mM) in CH_3CN with $[(n\text{-}Bu)_4N]ClO_4$ as supporting electrolyte when $Pb(ClO_4)_2$ is added from 0 (blue) to 1 equiv (deep red).

Receptor **2** also showed a perturbation of the oxidation wave in the presence of Zn^{2+} and Hg^{2+} ions although to a lesser extent. Upon addition of small amounts of these metal cations, a new oxidation wave at $E_{1/2} = 0.68$ V ($\Delta E_{1/2} = 90$ mV) for Zn^{2+} cations and $E_{1/2} = 0.71$ V ($\Delta E_{1/2} = 120$ mV) for Hg^{2+} cations anodically shifted appeared. Remarkably, linear sweep voltammetry (LSV) studies carried out upon addition of Cu^{2+} to a CH_3CN solution of ligand **2** showed a significant shift of the sigmoidal voltammetric wave toward cathodic currents, indicating that this metal cation promotes the oxidation of the free receptor. The presence of Li^+, Na^+, K^+, Ca^{2+}, Mg^{2+}, Ni^{2+}, and Cd^{2+} metal cations had no effect on neither OSWV nor CV of the receptor **2**, even when present in large excess. Interestingly, receptor **3** exhibited the highest selectivity toward metal cations because only in the presence of Pb^{2+} cations the oxidation wave of the ferrocene/ferrocenium redox couple was anodically shifted from $E_{1/2} = 0.64$ V to $E_{1/2} = 0.76$ V ($\Delta E_{1/2} = 120$ mV). Remarkably, these electrochemical results indicate that smaller potential shift of the monosubstituted receptor upon Pb^{2+} complexation (**3** < **2** < **1**) corresponds to higher selectivity in the recognition properties of the receptor (**3** > **2** > **1**).

Two-armed ferrocene derivatives **4** and **5** also exhibit selectivity toward Pb^{2+} and Zn^{2+} over the tested metal cations. The oxidation potential of the bis(imidazopyridine)ferrocene **4** is only shifted by addition of 1 equiv of Pb^{2+} ($\Delta E_{1/2} = 180$ mV) and Zn^{2+} ($\Delta E_{1/2} = 190$ mV) metal cations. Addition of Cu^{2+} induced oxidation of the ferrocene/ferrocenium redox couple, as indicated by the shift toward cathodic currents of the sigmoidal voltammetric wave, when LSV experiments were carried out in the presence of variable amounts of this metal cation (see Supporting Information). The same electrochemical behavior is found in the bis(imidazophenazine)ferrocene **5**, which undergoes perturbation of the oxidation potential in the presence of Pb^{2+} ($\Delta E_{1/2} = 110$ mV) and Zn^{2+} ($\Delta E_{1/2} = 170$ mV) metal cations. The electrochemical changes observed in the two-armed ferrocenes **4** and **5** upon complexation show that the potential shift is higher for Zn^{2+} ions than Pb^{2+} ions, which is in clear contrast to those observed for the monoarmed ferrocenes **2** and **3**. In this context, it has been reported[32] that 1,1′-disubstituted ferrocenes undergo a large anodic redox shift

of the ferrocene/ferrocenium redox couple upon complexation with Zn^{2+} metal cations.

The metal recognition properties of the receptors **1**−**5** toward the above-mentioned set of metal cations were also evaluated by UV−vis spectroscopy. Titration experiments for CH_3CN solutions of receptors ($c = 1 \times 10^{-4}$ M) and the corresponding aqueous metal cation solutions ($c = 2.5 \times 10^{-2}$ M) were performed and analyzed quantitatively.[33] Regarding the receptor **1**, addition of aqueous Pb^{2+} introduced as perchlorate induced a small red shift of the LE band by $\Delta\lambda = 15$ nm, similar to those observed ($\Delta\lambda = 11$ nm) when Zn^{2+} or Hg^{2+} ions were added. The most prominent features observed in the UV−vis spectrum of receptor **2** upon addition of successive substoichiometric amounts of aqueous Pb^{2+} are a progressive red shift of the HE band ($\Delta\lambda = 11$ nm) and LE band ($\Delta\lambda = 44$ nm). These changes occur at around one isosbestic point at 315 nm, at any receptor/Pb^{2+} ratio, suggesting that only one spectral distinct complex was present. These facts are responsible for a perceptible change of color from colorless to orange, which can be used for the "naked eye" detection of this divalent cation. Accurate values of the association constant (K_a) were determined using standard UV titration methods. The binding isotherms were generated by recording the changes in the UV absorption as a function metal cation concentration. Binding assays using the method of continuous variations (Job's plot) are consistent with a 1:1 binding stoichiometry. The data were well fitted to a 1:1 binding isotherm, and the association constant was calculated: $K_a = 3.3 \times 10^5$ M^{-1}. The HE and LE bands were also red-shifted (6−11 and 29−34 nm, respectively), although without any change of color upon addition of Zn^{2+} ($K_a = 1.4 \times 10^4$ M^{-1}) and Hg^{2+} ions, and a well-defined isosbestic point at $\lambda = 318$ nm was also observed.

The absorption spectrum of the imidazophenazine−ferrocene dyad **3** displays noticeable changes only in the presence of aqueous Pb^{2+} cations. Thus, addition of increasing amounts of Pb^{2+} cations to a solution of receptor **3** caused a progressive appearance of a new strong band located at 404 nm ($\varepsilon = 20\,500$ M^{-1} cm^{-1}) and a red shift of the LE band from 503 nm ($\varepsilon = 5700$ M^{-1} cm^{-1}) to 526 nm ($\varepsilon = 5600$ M^{-1} cm^{-1}) (Figure 2). Two well-defined isosbestic points at $\lambda = 433$ and 510 nm were found, indicating that a neat interconversion between the uncomplexed and complexed species occurs. The new LE band is red-shifted by 23 nm and is responsible from the change of color from pale orange to red. Remarkably, no changes were observed in the absorption spectrum of **3** after addition of Zn^{2+} and Hg^{2+} ions. The resulting Job plot suggests a 2:1 binding model, the global association constant being $\beta = 3 \times 10^8$ M^{-2} for Pb^{2+} and $\beta = 1.5 \times 10^8$ M^{-2} for Zn^{2+} (error <10%).

Addition of increasing amounts of Pb^{2+} ions to a solution of the two-armed imidazopyridine ferrocene **4** caused a red shift of the low energy band by $\Delta\lambda = 23$ nm, which is responsible from the change of color from colorless to yellow. Two well-defined isosbestic points at 311 and 329 nm indicate that a neat interconversion between the uncomplexed and complexed species occurs. Binding assays using the method of continuous variations (Job's plot) suggest a 1:1 binding model with a $K_a = 1.4 \times 10^5$ M^{-1}. The low energy band of the receptor **4** was also red-shifted ($\Delta\lambda = 7$ nm) upon addition of Zn^{2+} ($K_a = 8.3 \times 10^4$ M^{-1}), and two well-defined isosbestic point at 316 and 337 nm were also observed. The absorption spectrum of receptor **5** in the presence Pb^{2+} and Zn^{2+} ions underwent a slight blue shift of the low energy band ($\Delta\lambda = 7$ nm) and, more important, a dramatic blue shift of the high energy band ($\Delta\lambda = 160$ nm), whereas the band located at 397 nm remained unchanged. Two well-defined isosbestic points around 490 and 350 nm are present. From the titration data, a 1:1 binding mode is deduced and the association constant were found to be $K_a = 3.5 \times 10^3$ M^{-1} for Pb^{2+} and $K_a = 6.2 \times 10^3$ M^{-1} for Zn^{2+} ions.

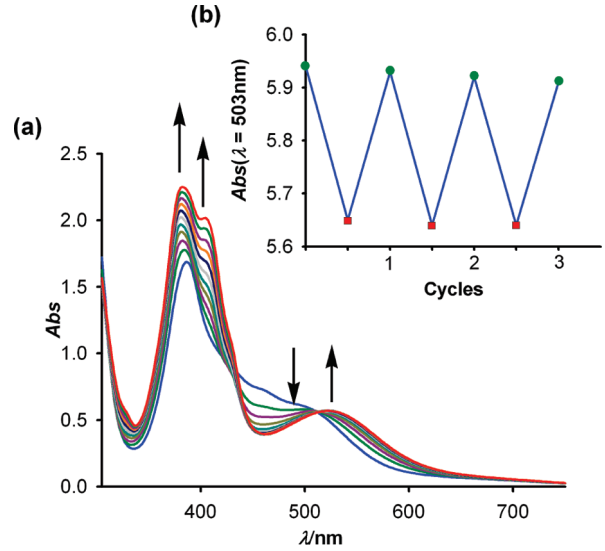

FIGURE 2. (a) Changes in the absorption spectra of receptor **3** ($c = 0.1$ mM) in CH_3CN upon addition of increasing amounts of Pb^{2+}. Arrows indicate the absorptions that increase or decrease during the experiment. (b) Changes observed at $\lambda = 526$ nm (complexation of receptor **3** with Pb^{2+}) and at $\lambda = 503$ nm (decomplexation with ethylenediamine).

These absorption spectral data reveal that the highest sensitivity is associated with the presence of an imidazopyridine arm in the receptor **2**, whereas the imidazophenazine ring in receptor **3** induced the highest selectivity toward Pb^{2+} cations. Regrettably, the awaited benefit, in terms of selectivity and/or sensitivity, by increasing the number of binding sites in the two-armed ferrocenes **4** and **5** was not found.

The fluorescent behavior of these receptors, in the presence of the above-mentioned set of metal cations, was also examined. While receptor **1** in CH_3CN did not undergo any considerable change in its emission spectra, upon addition of all the divalent metal cations used, receptor **2** showed a large CHEF (chelation-enhanced fluorescence)[34] effect when aqueous Pb^{2+} cation was added and a relatively small CHEF effect upon addition of Zn^{2+} (Figure 3). From the fluorescence titrations, the association constants for Pb^{2+} and Zn^{2+} were calculated to be $K_a = 6.1 \times 10^5$ and 2.7×10^4 M^{-1}, respectively. Overall emission changes of 620- and 150-fold were observed for Pb^{2+} and Zn^{2+}. Moreover, the increases in quantum yield of **2** induced by Pb^{2+} ($\Phi = 4.31 \times 10^{-2}$) and Zn^{2+} ($\Phi = 1.37 \times 10^{-2}$) ions were 110- and 35-fold, respectively. The effect of the different binding between the one-arm ligand **2** and the two-arm ligand **4** is shown by comparison of the different fluorescent behavior of both ligands upon complexation (Figure 3).

(32) Zapata, F.; Caballero, A.; Espinosa Tárraga, A.; Molina, P. *Org. Lett.* **2007**, *9*, 2385–2388.

(33) Association constants were obtained using the computer program Specfit/32 Global Analysis System, 1994−2004 Spectrum Software Associates (SpecSoft@compuserve.com). The Specfit program was acquired from Bio-logic SA (www.bio-logic.info) in January 2005.

(34) CHEF is defined as the I_{max}/I_0, where I_{max} corresponds to the maximum emission intensity of the receptor−metal complex, while I_0 is the maximum emission intensity of the free receptor.

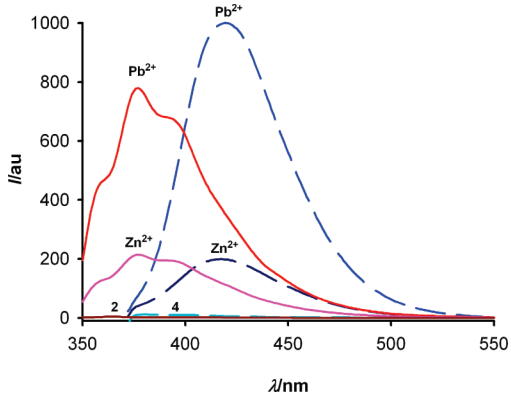

FIGURE 3. Changes in the fluorescence spectra of receptor **2** (deep red) and **4** (cyan) ($c = 1 \times 10^{-5}$ M) in CH_3CN upon addition of 1 equiv of Pb^{2+} or Zn^{2+} metal cations.

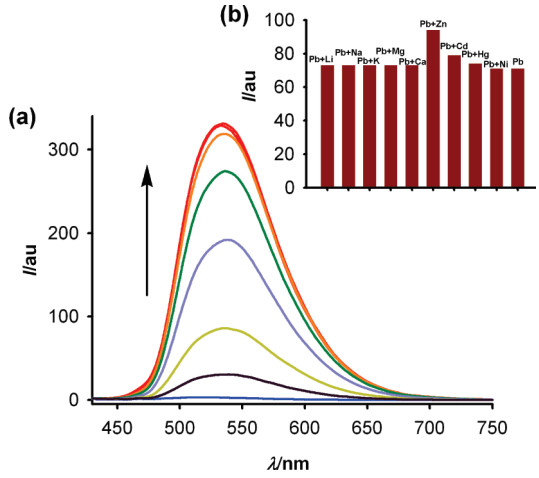

FIGURE 4. (a) Changes in the fluorescence spectra of **3** (1×10^{-5} M) in CH_3CN upon addition of Pb^{2+} ion. (b) Fluorescence emission intensity of **3** upon addition of 0.5 equiv of Pb^{2+} in the presence of 0.5 equiv of background metal ions in H_2O.

The addition of 1 equiv of Pb^{2+} to a solution of the receptor **4** in the same solvent induced a red shift of the emission band from 379 to 418 nm ($\Delta\lambda = 39$ nm) accompanied by a remarkable increase of the intensity of the emission band (CHEF = 181), and the quantum yield ($\Phi = 0.350$) resulted in a 890-fold increase. In the presence of 1 equiv of Zn^{2+} ions, an increase of the intensity of the emission band (CHEF = 36) and the quantum yield ($\Phi = 0.100$) was observed (Figure 4). From the fluorescence titrations, the association constants for Pb^{2+} and Zn^{2+} were calculated to be $K_a = 4.1 \times 10^6$ and 1.6×10^5 M^{-1}, respectively. For both imidazopyridine−ferrocene-based receptors, the selectivity for Pb^{2+} was more than 20 times that for Zn^{2+}. In addition, it should be noted that high sensitivity for Pb^{2+} is achieved by the receptor **2** in the present study. The detection limit, calculated as three times the standard deviation of the background noise, is unprecedented, and it was found to be 1.32×10^{-8} M (2.7 μg L^{-1}), which is lower than the maximum permitted amount of Pb^{2+} in drinking water defined by World Health Organization.

For receptor **3**, fluorescent titration experiments demonstrate that only Pb^{2+} and Zn^{2+} cations yielded progressively an intense enhancement of the emission band at 535 nm, CHEF = 133 for Pb^{2+} and 74 for Zn^{2+}. The stoichiometry of the complexes was also determined by the changes in the fluorogenic response of receptor **3** in the presence of varying concentrations of these

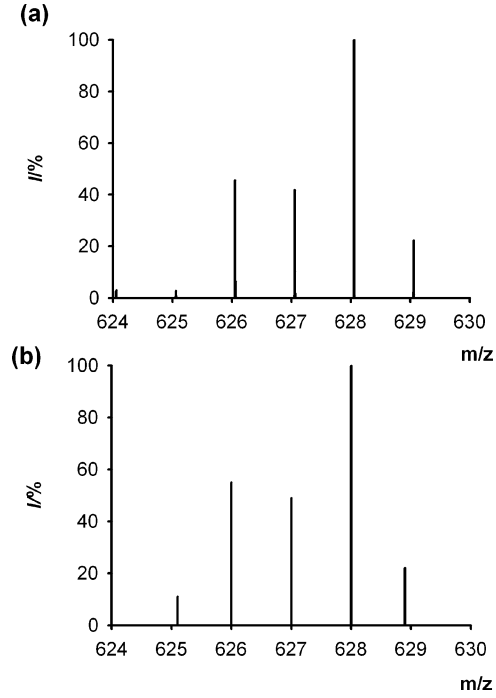

FIGURE 5. (a) Experimental relative abundance of the isotopic cluster for **4**·Pb^{2+} and (b) simulated.

metal cations, and the results obtained indicate the formation of 2:1 complexes, being the global association constants of $\beta = 5.9 \times 10^9$ M^{-2} for Pb^{2+} and $\beta = 4.5 \times 10^9$ M^{-2} for Zn^{2+}. On the other hand, the calculated detection limits were 2.5×10^{-6} and 2.4×10^{-6} M, respectively. The increases in quantum yield of **3** induced by Pb^{2+} ($\Phi = 0.487$) and Zn^{2+} ($\Phi = 0.306$) ions were 840- and 530-fold, respectively. The interference in the selective response of receptor **3** in the presence of Pb^{2+} from the other metal cations tested was also studied by using cross-selectivity experiments (Figure 4b).

After addition of 1 equiv of Pb^{2+} ions to a solution of the receptor **5** in CH_3CN, the emission band was red-shifted by 10 nm, increased by a CHEF = 220, and the fluorescence quantum yield increased by a factor of 63 ($\Phi = 0.075$). Similar but smaller changes were observed in the presence of Zn^{2+} ($\Phi = 0.013$, 11-fold) and CHEF = 97. The stoichiometry of the complexes was also determined by the changes in the fluorogenic response of **5** in the presence of varying concentrations of Pb^{2+} and Zn^{2+}, the results indicating the formation of 1:1 complexes with association constants $K_a = 1.5 \times 10^5$ M^{-1} for Pb^{2+} and $K_a = 9.5 \times 10^4$ M^{-1} for Zn^{2+} and detection limits 4.5×10^{-6} and 4.3×10^{-6} M, respectively.

The binding modes proposed from absorption and fluorescent data were further confirmed by electrospray mass spectrometry in the presence of the metal cations. The ESI-MS spectrum of receptor **2** in the presence of Pb^{2+} ions shows a peak at *m*/*z* 510 corresponding to the 1:1 complex. The relative abundance of the isotopic cluster was in good agreement with the simulated spectrum of the [**2**·Pb^{2+}] complex. In addition, a peak at *m*/*z* 609 corresponding to the [**2**·Pb + (ClO_4)]$^+$ also appeared. Likewise, receptor **4** also showed a peak at *m*/*z* 628 corresponding to the [**4**·Pb^{2+}] (Figure 5). In the case of receptor **3**, a peak at *m*/*z* 1012 corresponding to the complex 2:1 [$\mathbf{3}_2$·Pb^{2+}] is present (see Supporting Information). This binding mode is also confirmed for Zn^{2+} ions by the appearance of a peak at *m*/*z* 871 due to the complex [$\mathbf{3}_2$.Zn^{2+}] (see Supporting Information).

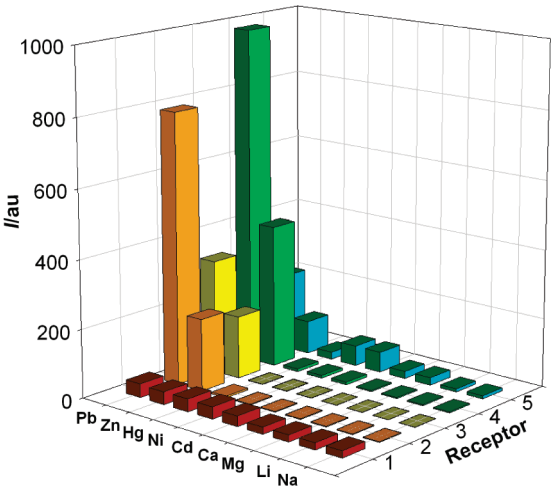

FIGURE 6. Increase of the fluorescent emission intensity of ligands **2** (red), **3** (orange), **4** (yellow), and **5** (green) in CH_3CN, after addition of 1 equiv of several cations.

Similarly, the ESI-MS spectra obtained by addition of Pb^{2+} and Zn^{2+} metal cations to the two-armed receptor **5** show the presence of peaks at $m/z = 829$ and 687, respectively, indicating that formation of [**5**·Pb^{2+}] and [**5**·Zn^{2+}] complexes also takes place.

The high selective binding ability of receptors **2**−**5** for Pb^{2+} over other mono- and divalent metal ions was tested, which was also investigated by competition-based fluorescence experiments (Figure 6). The selectivity of ferrocene derivatives **2**−**5** for Pb^{2+} over Ca^{2+}, Cd^{2+}, and Hg^{2+} is particularly important because Pb^{2+} targets Ca^{2+}-binding sites in vivo[35] and Cd^{2+} and Hg^{2+} are metal cations that frequently interfere with Pb^{2+} analysis.

^{1}H NMR experiments were performed to explore the coordination mechanism of receptors **2**−**5** and Pb^{2+} ions (Figure 7). The complexation process of receptor **2** in CD_3CN induces not only noticeable downfield changes in the chemical shifts in the pyridine ring protons ($\Delta\delta$ = 0.13−0.39 ppm) but also relatively large downfield shifts in the ferrocene protons ($\Delta\delta$ = 0.12−0.27 ppm). Addition of 1 equiv of Zn^{2+}, however, induces only downfield shifts in the pyridine ring protons, whereas Hg^{2+} metal ions caused a broadening of all peaks in the ^{1}H NMR spectrum, from which not accurate chemical shifts could be obtained. Due to low solubility of receptor **4**, the complexation process was carried out in deuterated methanol, and only in the presence of Pb^{2+} ions, both the pyridine ring protons and the cyclopentadienyl protons are downfield shifted by around 0.1 ppm.

The structural characterization of the interaction process between the receptor **3** and Pb^{2+} ions was examined in acetone-d_6 (Figure 7). A cursory glance of ^{1}H NMR spectral change after addition of increasing amounts of Pb^{2+} ions reveals that the resonance ascribable to the NH proton of receptor **3** (δ = 11.88 ppm) completely disappeared. Simultaneously, the two singlets corresponding to the two protons of the central benzene ring (δ = 8.33 and 8.07 ppm) collapsed in only one shifted singlet at δ = 8.46 ppm ($\Delta\delta$ = +0.13 and + 0.39 ppm). Moreover, the two multiplets corresponding to the four protons of the peripheral benzene ring also were downfield shifted ($\Delta\delta$ = +0.07 and + 0.14 ppm) although to less extent. Similar behavior was also observed for the protons present in the ferrocenyl moiety, although the magnitude of these downfield shifts are considerable larger: $\Delta\delta$ = +0.26 and + 0.38 ppm for the two pseudotriplets associated with the protons in the monosubstituted Cp ring, and $\Delta\delta$ = +0.22 for the singlet corresponding to the protons within the unsubstituted Cp ring. The noticeable spectral changes of the central benzene ring protons as well as the ferrocenyl protons could indicate that the five-membered imidazole ring is acting as an effective binding site in the complexation event.

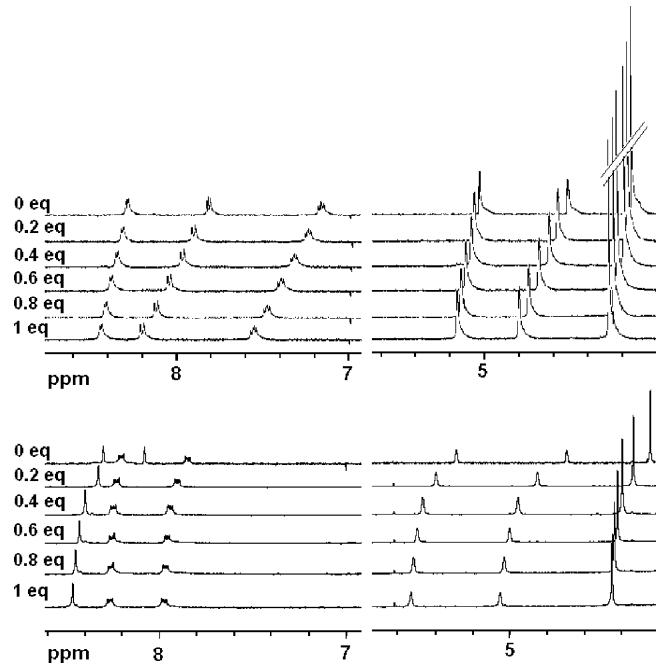

FIGURE 7. Evolution of the ^{1}H NMR spectra of **2** in CD_3CN (top) and **3** in acetone-d_6 (bottom) upon addition of increasing amounts of Pb^{2+}, from 0 to 1 equiv.

Upon addition of Pb^{2+} metal cations to a colorless solution of **2** in CH_3CN, both an orange color and a strong fluorescence appear. The turn-on response is reversible because both signals disappear upon the addition of an excess of cyclen or ethylenediamine. Furthermore, a CH_2Cl_2 solution of the complex **2**·Pb^{2+} was treated with an ethylenediamine aqueous solution, and the absorption, ^{1}H NMR spectra, and CV of the extracted product were identical to those of free receptor **2**. Formation of the complex **2**·Pb^{2+} and the subsequent extraction of the metal cation with ethylenediamine were carried out over several cycles. The optical and emission spectra were recorded after each step and found to be fully recovered on completion of the step, thus, demonstrating the high degree of reversibility of the sensing process.

This kind of complexation/decomplexation study was also carried out with receptors **3**−**5**, and in all cases, the observed behavior was the same as that found for receptor **2**.

DFT-based quantum chemical calculations have provided the required insight into the nature of binding of the receptors herein studied toward metal cations. In this regard, some specific DFT methods have proved quite useful for studying systems with noncovalent interactions, offering an electron correlation correction frequently comparable or, in certain cases and for certain purposes, even superior to MP2, but at considerably lower

(35) (a) Goldstein, G. W. *Neurotoxicology* **1993**, *14*, 97–102. (b) Simons, T. J. B. *Neurotoxicology* **1993**, *14*, 77–86. (c) Goyer, R.-A. *Environ. Health Perspect.* **1990**, *86*, 177–182.

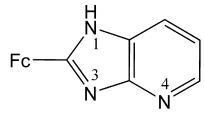

2-Ferrocenyl-1*H*-imidazo[4,5-*b*]pyridine

2

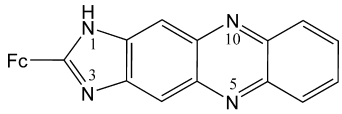

2-Ferrocenyl-1*H*-imidazo[4,5-*b*]phenazine

3

computational cost.[36] We have used Truhlar's hybrid meta functional mPW1B95[37] that has been recommended for general purpose applications and was developed in order to produce a better performance where weak interactions are involved such as those between ligands and heavy metals.[38] At the working level of theory, **2** is the most stable of the two possible tautomers and forms a moderately stable complex with $Pb(ClO_4)_2$ in acetonitrile ($\Delta E_{MeCN} = -9.63$ kcal·mol^{-1}). Although in solution the perchlorate counteranions could be partially or totally displaced to a second coordination sphere by the coordinating solvent (acetonitrile) molecules, we have used a [**2**·$Pb(ClO_4)_2(CH_3CN)_2$] species as model for the complexation product, provided that it is expected to constitute an acceptable approximation to the binding of the large Pb^{2+} cation to receptor **2**. The deazapurine ligand **2** provides only one strong linkage to the Pb^{2+} ion through the pyridine-like N-4 atom ($d_{Pb-N} =$ 2.565 Å, WBI 0.190, $r(r_{c[N4-Pb]}) = 3.09 \times 10^{-2}$ au), whereas the other imidazole-like N-3 atom is weakly bound ($d_{Pb-N} =$ 3.037 Å, WBI 0.098, $\rho(r_{c[N3-Pb]}) = 1.41 \times 10^{-2}$ au) (Figure 8). We have also used the Bader's AIM (atoms-in-molecules) methodology[39] to perform a topological analysis of the electronic charge density $\rho(r)$ in order to search for significant bond critical points (BCPs) around the spatial region where the host−guest interactions are taking place. According to this theory, when two neighboring atoms are chemically bound, a BCP appears between them. The electron densities of the BCPs for the above-mentioned Pb^{2+}−acetonitrile interactions correlate with the proposed bond strength ($\rho(r_{c[N4-Pb]}) = 3.09 \times 10^{-2}$ au > $\rho(r_{c[N3-Pb]}) = 1.41 \times 10^{-2}$ au). In addition, four coordination positions are occupied by one strongly bound and other weakly interacting O atom in every perchlorate unit, and two additional weakly coordinating CH_3CN ligands are explicitly added in order to complete an eight-coordination sphere around the big Pb^{2+} metal cation.[40] Furthermore, the sign of the Laplacian of the electron density at a bond critical point, $\nabla^2\rho(r_c)$, reveals whether the charge is concentrated, as in covalent bonds ($\nabla^2\rho(r_c) < 0$), or depleted, as in closed shell (electrostatic) interactions ($\nabla^2\rho(r_c) > 0$).[41] In the **2**·$Pb(ClO_4)_2(CH_3CN)_2$ complex, only the strongest metal−ligand interactions with the azapurine N-4 atom and one of the O atoms exhibit small negative $\nabla^2\rho(r_c)$ values characteristic for moderately covalent bonds.[42] On the other hand, a plausible 2:1 ligand−metal stoichiometry was ruled out on the basis of the lower stability (by 11.26 kcal·mol^{-1} in the gas phase) of the resulting **2**$_2$·$Pb(ClO_4)_2$ complex.

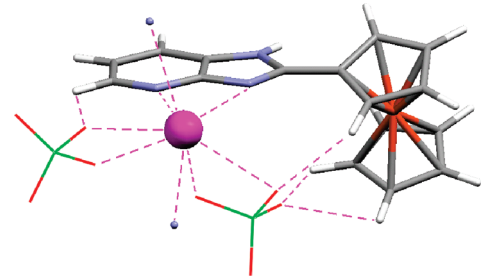

FIGURE 8. Calculated structure for the **2**·$Pb(ClO_4)_2(CH_3CN)_2$ complex. Perchlorate anions are represented in wireframe, and only acetonitrile donor N atoms (small blue spheres) are sketched for clarity.

We assume that the resulting structure agrees with that obtained from ^{1}H NMR data because it explains that either the pyridine H-5 and the ferrocene Cp_1-Hα and Cp_2-H atoms are less deshielded due to the formation of hydrogen bonding with ligands (solvent or perchlorate anions) involved in the coordination sphere around the Pb^{2+} cation (Figure 8). A good agreement with the experimentally observed LE band in the absorption spectrum is also obtained from the TD-DFT calculation performed for the **2**·$Pb(ClO_4)_2(CH_3CN)_2$ complex that shows a significant allowed transition from HOMO and HOMO-1 to LUMO at 598.8 nm (not scaled) with moderately high oscillator strength ($f = 0.035$ au). This represents a remarkable bathochromic effect ($\Delta\lambda = +102.0$ nm) with respect to the analogous (HOMO/HOMO-1 → LUMO) LE transition in the free ligand **2**, which is mainly due to a comparative stabilization of the LUMO with respect to that experienced by the HOMOs (Figure 9).

In the case of the monoarmed imidazophenazine ferrocene receptor **3**, the absence of adjacent pairs of N atoms prevents it from acting as bidentate ligand. If no previous deprotonation occurs, **3** can behave as a monodentate N ligand through either imidazole N-3 or pyridine-like N-5 or N-10 atoms. Unlike **2**, according to our calculations, ligand **3** exhibits a remarkable preference to form a 2:1 ligand−metal complex with $Pb(ClO_4)_2$. Again, we believe that a **3**$_2$·$Pb(ClO_4)_2$ complex could acceptably account for the actual species, even if the coordinating acetonitrile molecules of the solution could displace the perchlorate anions to an outer coordination sphere. The most stable of such **3**$_2$·$Pb(ClO_4)_2$ complexes resulted to be the one featuring the Pb^{2+} cation coordinated by the N-10 atom ($\Delta E_{MeCN} = -50.38$ kcal·mol^{-1}) (Figure 10), whereas formation of the most stable 1:1 complex through the N-3 donor atom **3**·$Pb(ClO_4)_2(CH_3CN)_2$ was found to be slightly endergonic ($\Delta E_{MeCN} = +0.53$ kcal·mol^{-1}). In the resulting minimum energy **3**$_2$·$Pb(ClO_4)_2$ complex, the Pb^{2+} cation is hexacoordinated by the N-10 atom of every ligand **3** and two pairs of similar perchlorate O atoms[43] in a centrosymmetric square pyramid environment.

It is worth mentioning that several other less stable minima were found for **3**$_2$·$Pb(ClO_4)_2$ species, in which the Pb^{2+} cation

(36) Rablen, P. R.; Lockman, J. W.; Jorgensen, W. L. *J. Phys. Chem. A* **1998**, *102*, 3782–3797.

(37) (a) Zhao, Y.; Truhlar, D. G. *J. Phys. Chem. A* **2004**, *108*, 6908–6918. (b) Zhao, Y.; Truhlar, D. G. *J. Phys. Chem. A* **2005**, *109*, 5656–5667.

(38) For instance, see: Muñiz, J.; Sansores, L. E.; Martínez, A.; Salcedo, R. *J. Mol. Struct.* **2007**, *820*, 141–147.

(39) Bader, R. F. W. *Atoms in Molecules: A Quantum Theory*; Oxford University Press: Oxford, 1990.

(40) Perchlorate O donor atoms: $d_{Pb-O} = 2.498$, 2.523, 2.905, and 2.979 Å; WBI 0.169, 0.165, 0.084, and 0.073; $\rho(r_{c[O-Pb]}) = 2.98 \times 10^{-2}$, 2.87×10^{-2}, 1.73×10^{-2}, and 1.53×10^{-2} au. Acetonitrile N donor atoms: $d_{Pb-N} = 2.851$ and 2.977 Å, WBI 0.118 and 0.105, $\rho(r_{c[N-Pb]}) = 1.90 \times 10^{-2}$ and 1.57×10^{-2} au.

(41) Nakanishi, W.; Nakamoto, T.; Hayashi, S.; Sasamori, T.; Tokitoh, N. *Chem.—Eur. J.* **2007**, *13*, 255–268, and references cited therein.

(42) Ligand **2**: $\nabla^2\rho(r_{c[N4-Pb]}) = -0.866 \times 10^{-2}$ au; $\nabla^2\rho(r_{c[N3-Pb]}) = 2.608 \times 10^{-2}$ au. Perchlorate O atoms: $\nabla^2\rho(r_{c[O-Pb]}) = -0.772 \times 10^{-2}$, 0.135×10^{-2}, 2.863×10^{-2}, and 2.747×10^{-2} au. $CH_3C\underline{N}$: $\nabla^2\rho(r_{c[N-Pb]}) = 2.981 \times 10^{-2}$ and 2.902×10^{-2} au.

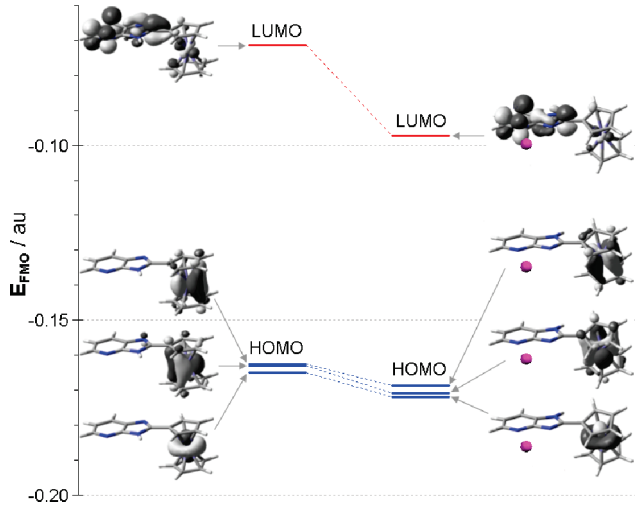

FIGURE 9. Calculated MO diagram (in au) for ligand **2** (left) and complex **2**·Pb$(ClO_4)_2(MeCN)_2$ (right). Perchlorate and acetonitrile ligands are omitted for clarity.

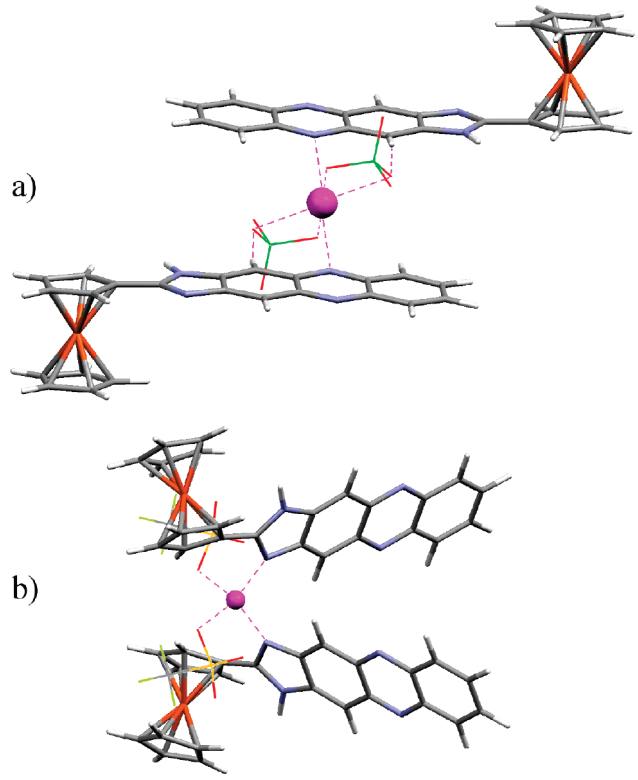

FIGURE 10. Calculated structure for complexes (a) **3₂**·Pb$(ClO_4)_2$ and (b) **3₂**·Zn$(OTf)_2$. Perchlorate and triflate anions are represented in wireframe for clarity.

is π-bonded to the inner carbocyclic ring instead of being σ-bonded to N atoms. In the potential energy surface, the most stable of such π-bonded complexes is only 2.31 kcal·mol^{-1} above the absolute minimun previously described, from which can be derived upon little reorganization. It features a short η^3-type contact with the N10−C10a−C11 fragment belonging to ligand **3** (2.990, 3.200, and 3.054 Å, respectively), whose nature is evidenced by the moderately high bond ellipticity value (average $\varepsilon = 0.224$) that within the AIM methodology has been considered as a quantitative measure of the bond π-character. These types of "π-complexes" could be involved as intermediates in an isomerization process between N10 and N5 com-

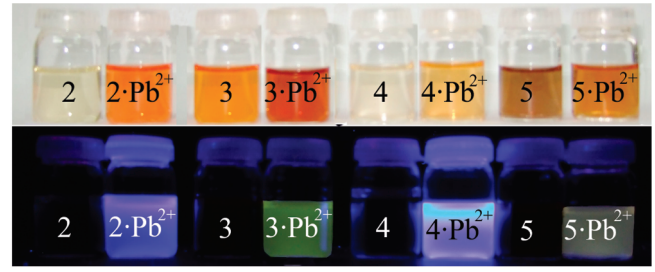

FIGURE 11. Visual features observed in CH_3CN solutions of receptors **2**−**5** and their corresponding complexes with Pb^{2+} ion: (top) absorptions; (bottom) emissions.

plexation modes, in combination with subsequent deprotonation−reprotonation processes, which would tentatively explain the high symmetry observed in the NMR spectrum of **3₂**·Pb$(ClO_4)_2$ (Figure 7b).

Complexation of Zn$(OTf)_2$ was also predicted to occur with 2:1 ligand−metal stoichiometry involving in this case the heterocyclic N-3 atom, as far as the resulting C_2-symmetric **3₂**·Zn$(OTf)_2$ complex (Figure 10b) was found to be more stable ($\Delta E_{MeCN} = -26.87$ kcal·mol^{-1}) than the 1:1 complex **3**·Zn$(OTf)_2$ ($\Delta E_{MeCN} = -19.32$ kcal·mol^{-1}). The most stable complex features the Zn^{2+} cation in a tetrahedral environment made up by two identical N-3 atoms belonging to both imidazophenazine ligands and two identical triflate O atoms[44]

Conclusion

In summary, the synthesis of new ferrocenyl azaheterocycle multichannel chemosensor molecules **2**−**5** has been achieved in a short synthetic sequence from commercial starting materials. The structurally simple and easily synthesized mono- and two-armed ferrocenes **2**−**5** not only display a strong interaction between the azaheterocycle ring and Pb^{2+} ions but also distinguish by electrochemical and spectroscopic (absorption, emission, and ^{1}H NMR) techniques this metal cation from other metal ions, including the strong competitors Ca^{2+}, Cd^{2+}, and Hg^{2+}. Receptors **2**−**5** represent the first example of a Pb^{2+} multichannel chemosensor molecule, which combines redox detection ($\Delta E_{1/2} = 110-180$ mV) and the sensitivity of fluorescence (detection limit of **2** = 2.7 μg L^{-1}) with the convenience of colorimetric assays, which allow the potential for "naked eye" detection (Figure 11).

Experimental Section

General Procedure for the Preparation of Compounds 1−5. To a solution of the appropriate 1,2-diamino compound (2.37 mmol) in nitrobenzene (5 mL) was added the corresponding ferrocenecarboxaldehyde (2.37 mmol) or ferrocenedicarboxaldehyde (1.19 mmol). Then, acetic acid (0.5 mL) was added, and the mixture was stirred at 60 °C for 15 h. The resulting orange solid was filtered, washed with diethyl ether (10 mL), chromatographed on a silica gel column using CH_2Cl_2/MeOH (9:1) as eluent, and, finally, crystallized from acetonitrile to give **1**−**5** as crystalline solids.

2-Ferrocenyl-1*H*-benzo[*d*]imidazole, 1: Prepared from 1,2-diaminobenzene and formylferrocene; 80% yield; mp > 300 °C; ^{1}H

(43) Ligand **3**: $d_{Pb-N} = 2.766$ Å, WBI 0.172, $\rho(r_{c[N3-Pb]}) = 2.59 \times 10^{-2}$ au, $\nabla^2\rho(r_{c[N3-Pb]}) = 2.19 \times 10^{-2}$ au. Perchlorate O atoms: $d_{Pb-O} = 2.657$ and 2.657 Å, WBI 0.145 and 0.140, $\rho(r_{c[O-Pb]}) = 2.64 \times 10^{-2}$ and 2.69×10^{-2} au, $\nabla^2\rho(r_{c[O-Pb]}) = 2.37 \times 10^{-2}$ and 2.33×10^{-2} au, respectively.

(44) Ligand **3**: $d_{N3-Zn} = 2.021$ Å, WBI 0.177, $\rho(r_{c[N3-Zn]}) = 7.96 \times 10^{-2}$ au, $\nabla^2\rho(r_{c[N3-Zn]}) = 38.27 \times 10^{-2}$ au. Triflate O atoms: $d_{O-Zn} = 2.002$ Å, WBI 0.130, $\rho(r_{c[O-Zn]}) = 7.18 \times 10^{-2}$ au, $\nabla^2\rho(r_{c[O-Zn]}) = 41.38 \times 10^{-2}$ au.

NMR (CD_6CN) δ 4.09 (s, 5H), 4.44 (st, 2H), 4.94 (st, 2H), 7.16 (m, 2H), 7.43 (m, 1H), 7.53 (m, 1H), 10.5 (br s, 1H); ^{13}C NMR (DMSO-d_6) δ 67.66, 69.72, 70.08, 74.60, 110.8, 118.2, 121.6, 135.1, 144.1, 153.3; MS (FAB^+) *m*/*z* (relative intensity) 303 ($M^+ + 1$, 100). Anal. Calcd for $C_{17}H_{14}FeN_2$: C, 67.58; H, 4.67; N, 9.27. Found: C, 67.35; H, 4.40; N, 9.05.

Acknowledgment. We gratefully acknowledge the financial support from MICINN-Spain, Project CTQ2008-01402, and Fundación Séneca (Agencia de Ciencia y Tecnología de la Región de Murcia) project 04509/GERM/06 (Programa de Ayudas a Grupos de Excelencia de la Región de Murcia, Plan Regional de Ciencia y Tecnología 2007/2010). A.C. also thanks the Ministerio de Educación y Ciencia for a predoctoral grant.

Supporting Information Available: NMR spectra; electrochemical, UV−vis, and fluorescence data; Job's plot; reversibility experiments; semilogarithmic plots for determining the detection limits; experimental section (general comments and characterization data of compounds **2**−**5**); and calculated structures. This material is available free of charge via the Internet at http://pubs.acs.org.

JO900533X